Application of Wavelet Transform to Identify Faulty IGBTs in 3-phase Induction Motor Drives

B.Sindhuja, Yarlagadda Gouthami

Department of Electrical and Electronics Engineering,

RMD Engineering College,

Kavarapettai, India

ABSTRACT—Switching Devices (IGBT) used in Pulse Width Modulation (PWM) Voltage Source Inverter (VSI) feeding an induction motor often suffers from different types of faults due to ageing or performance in unfriendly environments. These faults which are caused due to improper contact points, problematic solder joints, poor connections etc are often less severe at their initial stages. Different variations of the above mentioned faulty cases in a PWM VSI driven induction motor are simulated in PSIM software and results are diagnosed to estimate condition of the inverter. Three phase line currents feeding the motor are recorded and transformed to d-q reference frame using Park's Transformation for further analysis. From d and q current components thus obtained, the PVMs and PVACs are computed. Applying Continuous wavelet Transform on PVACs certain features are extracted which are helpful to distinguish healthy condition from faulty situations and segregates different cases of individual faulty IGBTs.

Keywords—PWM-VSI Drive; Park's Tranformation; Park's Vector Modulus(PVM); IGBT; Continuous Wavelet Transform; Scatter Plot

I. INTRODUCTION

IGBT based PWM–VSI motor drives are the most commonly used drive system in industries because of high current and voltage abilities of their power switching devices. But excessive electrical, thermal and environmental stresses during their operation can cause failures of these IGBT based drives. Early, reliable, and accurate identification of faulty components of drive module enables speedy repair and maintenance leading to large cost savings for industries.

IGBT failures can be broadly classified as open-circuit faults, short-circuit faults, and intermittent gate - misfiring faults. Total open circuit faults or partial open circuit faults are caused due to breakage of bonding wire because of thermal overheating or driver circuit malfunctioning [1, 2]. Spurious resistance arises in series with components at their terminals when cases of partial open circuit faults appear. These types of faults normally remains undetected and it leads to severe failure in other components such as overstressing of IGBTs and lead wires creating torque ripples in induction motor output [2, 3, 4]. It is thus important to study the effects of such faults in drive modules and find out ways to identify them.

Fault data in the form of phase voltages, d-q phase currents, obtained from model-based techniques [5] have been used to extract different features, which are implemented in expert systems [6] to diagnose and identify the faults**.** Stator Mean Current Vector is another approach used by authors of [7] to determine a pattern from where faulty IGBTs can be detected. Uses of a three-layer wavelet-neural network for identification of faults in inverter were reported in [8, 9].

In the present work, PWM -VSI driving an induction motor has been simulated in PSIM software by incorporating six types of faults into it. Each case is related with respective IGBTs having a resistance in series at their terminal aroused due to poor contacts. From the current signals obtained from faulty cases, Park's Vector Modulus (PVMs) are computed and features are extracted using CWT techniques to identify different types of faults.

VSI SYSTEM UNDER STUDY.

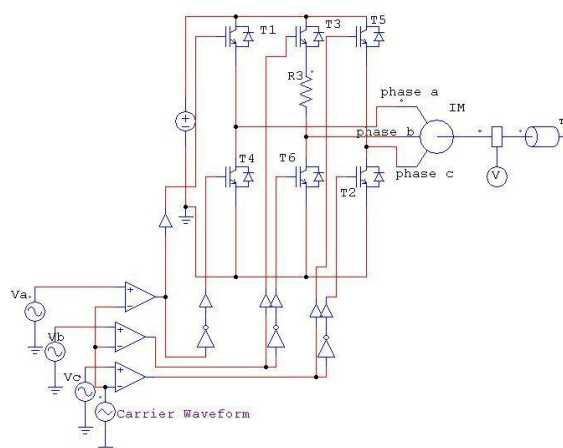Fig. 1 shows the PWM-VSI scheme which is under investigation.

Fig. 1. PWM-VSI scheme under study

Comparing with a practical induction motor of 1.5 KW, 440V rating, the setting of the parameters are done in the simulated scheme. Those setting are given in Table I and Table II respectively. One of the simulated faulty cases dealt in the present study are shown in the Fig. 1. As an example, the spurious resistance R3 caused due to improper soldering or due to aging is shown in series with IGBT T3. This brings distortion in the three- phase line currents

.

TABLE I.   CONTROL   CIRCUIT PARAMETERS

Setting of control circuit	Voltage (peak)	Frequency
Reference Sinusoidal Voltage	0.8V	50 Hz
Triangular Waveform (PWM Carrier)	1V	2KHz

TABLE II.   MOTOR PARAMETERS

Motor parameter	Values
Voltage	440V
power	1 .5 Kw
current	3. 3 amp
Speed	1432 rpm
Stator resistance	2.294 ohm
Stator inductance	0.139 H
Rotor resistance	2.156 ohm
Rotor inductance	0.0074 H

Similarly, other cases with poor drain terminal soldering of IGBTs and respective arousals of spurious resistance are listed in Table III.

TABLE CASES UNDER
III. STUDY

Case Study	Fault in drain terminal soldering in IGBT	Resistance representing faulty IGBT terminal
A	T1	R1
B	T2	R2
C	T3	R3
D	T4	R4
E	T5	R5
F	T6	R6
H	Healthy	

When these types of apparently innocent faults occur, the protective devices are not triggered. However, the three phase line currents become unbalanced and non-sinusoidal, indicating the presence of DC offset components in the output of the drives. Then the motor generates oscillating torque resulting in premature wearing of different mechanical parts such as shaft, bearings and so on. At the same time, the power switches in the drives and their respective terminals also falls under stress situation leading to further unpredictable failures. Fig. 2 shows the three-phase output current signature of the PWM drives when due to poor soldering or aging problem, a spurious resistance R3 has developed in the drain terminal of IGBT T3.
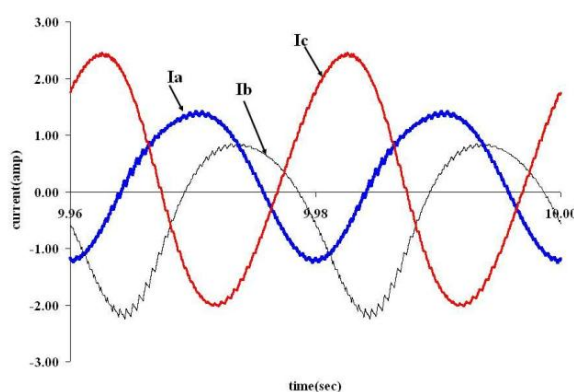
Fig. 2. Three phase line currents due to resistance in drain terminal of T3

III. BRIEF THEORY OF PARK'S TRANSFORMATION AND PARK'S VECTOR
    MODULUS

Using Park's Transformation approach, Induction motor three phase phenomena are converted to two dimensional (2-D) representations. Normally Induction motor PWM –drive does not have any neutral wire connection. Therefore, homo -polar components do not exist in the line. Then the 3-phase stator current equations are reducible to a set of two appropriate variables in a 2-phase reference frame (called the dq-

reference frame) [10]. The main phase current variables (Ia, Ib, Ic) are converted to Park's vector components (Id, Iq) using functions as represented in (1) and (2).

$$\sqrt{\frac{2}{3}} \quad \sqrt{\frac{1}{}} \quad \sqrt{\frac{1}{}} \qquad (1)$$

$$Id \; \square \; Ia \; -_6 Ib -\;_6 Ic$$
$$Iq \; \frac{1}{\square} \; \sqrt{\frac{1}{2}}Ib + \sqrt{\frac{1}{2}}Ic \qquad (2)$$

Park's Vector Modulus (PVM) are then computed as

$$PVM \; \square\sqrt{\quad Id^2 \; \square \; Iq^2} \qquad (3)$$

Analyzing the PVMs corresponding to the motor current signatures under different faulty conditions caused due to presence of spurious resistance at terminals of IGBTs, the affected IGBT can be identified.

IV.   ANALYSIS OF EXPERIMENTAL DATA

PVMs are computed using (3) for all the different faulty cases including the healthy case and plotted as shown in Fig. 3. From the figure, it is revealed that PVM plots have DC components superimposed by AC components. An ideal PVM plot of the stator current signature for a healthy case should have only DC component without any AC components. However, when faults occur a dominant AC component superimposes on the DC part along with some less dominant ripples [11].
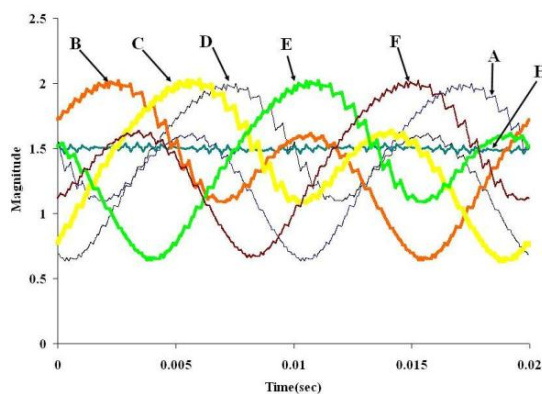

Fig. 5 and Fig. 6 shows the CWT spectrum of a healthy and faulty case (IGBT T3 having spurious resistance R3) obtained by applying the tools on corresponding PVACs signals. The translation values are taken as same value as that of no of data samples within one complete cycle. The multiple clusters of peaks shown in Fig. 5 are subdued and only a single significant cluster appears in Fig. 6.
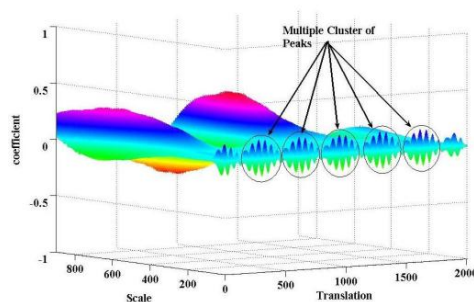

Fig. 3. PVMs corresponding to different cases as mentioned in Table-III

From the PVMs plot, the DC component is eliminated and only the AC parts are kept as shown in Fig. 4 and this plot is hereafter named as PVAC.
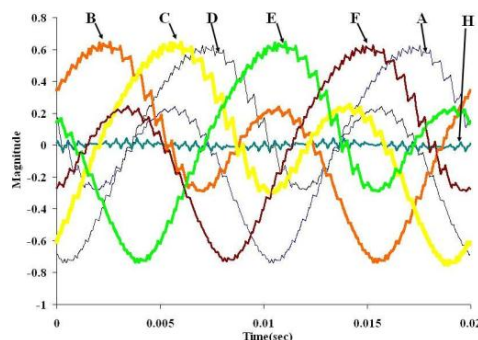

Fig. 4. PVACs corresponding to different cases as mentioned in Table-III

A. *Time Frequency Domain Analysis*

The non-stationary and periodic nature of the PVAC plots shown in Fig. 4 inspired the application of Continuous Wavelet Transform tools [11, 12]. The wavelet transform [13] of a function f(t) with respect to a mother wavelet ϕ is defined as

$$W_\phi \, f(b, a) = {}^{\alpha}\!\!\int f(t)\phi_{b,a}(t) \, dt \qquad (4)$$
$$-\alpha$$

$$\text{Where} \quad \phi_{b,a}(t) = \frac{1}{\sqrt{a}}\phi\left(\frac{t-b}{a}\right) \qquad (5)$$

The parameters b and a are called translation and scale parameters respectively. CWT plot of a time domain signal spreads over three axes, the x-axis represents position along the signal (time or translation), the y-axis represents scale (inverse of frequency), and the CWT coefficients are along the z-axis.

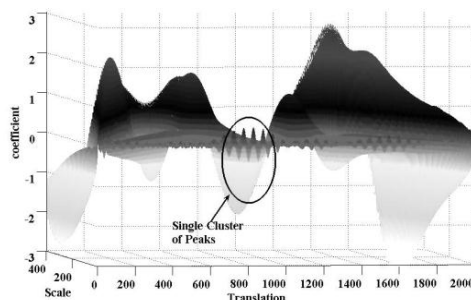Fig. 5. CWT spectra with healthy condition

Fig. 6. CWT spectra with IGBT T3 having a spurious resistance

B. Feature Extraction

The CWT spectra obtained shows the presence of several peaks having different translation, scale and coefficient values. These three parameters are important features to distinguish between healthy and faulty cases and to classify different faulty cases. Efficient clustering of fault features are enabled by dividing the entire range of CWT spectrum into three zones: low scale (high frequency), medium scale (medium frequency) and high scale (low frequency).

From the observation of the spectra it is determined that high scale zone is taken above scale value 90 and medium scale zone is taken between scale value 20 to 90 and scale value lower than 20 is taken as low scale zone. From Fig. 5 and Fig. 6 it is observed that global peak appears only at high scale zone for both healthy and faulty cases. But there are certain features that discriminate healthy from faulty situation.

- The global peak for healthy case has a much low coefficient value than the faulty cases.
- The scale value for global peak for healthy case is much high compared to that of the faulty cases though both the scale values fall in the high scale zone.

- For healthy case, in the mid-scale ranges, there are multiple clusters of peaks over the entire translation range (Fig. 5). But for faulty cases one significant cluster of peaks is observed at a particular region of translation values (Fig. 6). As shown in Fig. 7, there are four prominent peaks in the cluster mentioned above.
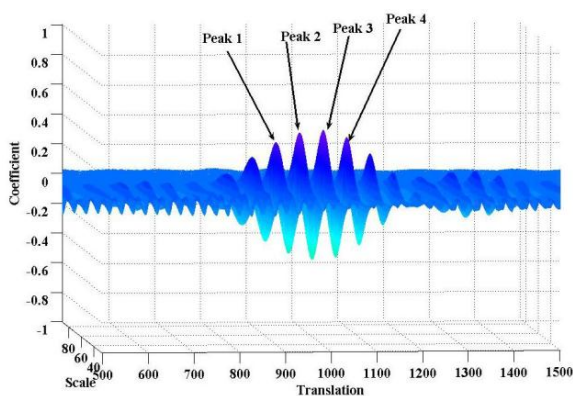

Fig. 7. Four dominant peaks in the medium scale region of CWT plot of PVAC for faulty situation in IGBT T3

Spurious resistances with values between 95 Ω to 105 Ω are simulated for each of the faulty cases and the corresponding coefficients of these four peaks are noted from CWT analysis. The coefficient values corresponding to different translation and scale values which are found to be most linear with respect to different tested spurious resistance values are selected as the effective feature along with their translation and scale values for discriminating different faulty cases. As an example, the PVAC signature of a faulty IGBT T3 having spurious resistances between 95 Ω to 105 Ω are analyzed with CWT toolbox and the per unit (pu) coefficients obtained for different values of resistances yet at similar values of translations and scales are plotted as shown in Fig. 8.
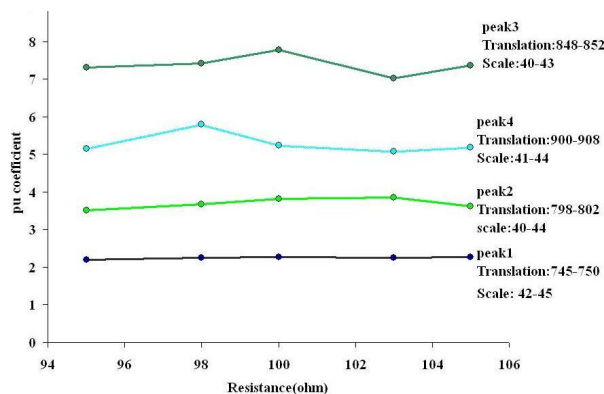
The pu coefficient values are obtained, by dividing the coefficient values of each fault case by the coefficient value of healthy case at that or nearest translation and scale value. It is found that pu coefficients for peak 1 are almost linear. So, pu coefficient values along with the respective translation and scale values are selected as effective features to distinguish the faulty IGBT T3. Similar extractions of appropriate features are done for all the other faulty IGBTs.

Low scale peaks are less significant compared to peaks at medium and high scale zones and so they are not studied.

C. Fault Discrimination

There are certain features, which distinguish, healthy from faulty cases but it is also essential to identify the particular IGBT, which is suffering from fault. 3-D Scatter plot gives a pictorial view of the variation of features with respect to faulty conditions occurring in different IGBTs. Fig. 9 shows 3 -D scatter plots of dominant peaks appearing in high scale zone of CWT corresponding to healthy and various fault conditions. It is clearly visible that the features locations of all faulty cases are totally secluded from that of the healthy case. However, this scatter plot is not sufficient to discriminate and identify the particular IGBT suffering from faulty conditions.
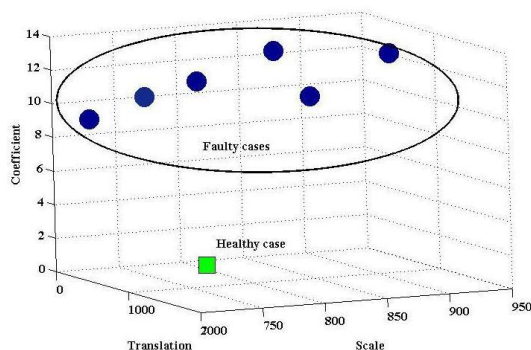

Fig. 9. 3-D scatter plots of dominant peaks in high scale zone corresponding to healthy and various fault conditions

In this regard, 3-D scatter in the mid scale Zone are studied and are plotted in Fig. 10.
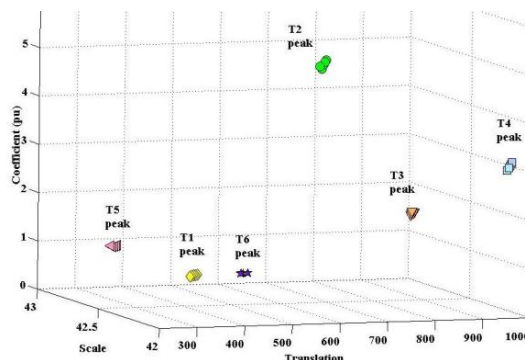
Fig. 8. Plot of pu Coefficients of the four dominant peaks w.r.t.different tested spurious resistances on IGBT T3

For each faulty IGBT five values of spurious resistance are taken into consideration. Thus, there are thirty different feature points in the 3-D scatter plots. These thirty different feature points are forming clusters into six groups marked as T1 peak to T6 peak as shown in the Fig. 10. Each of this group signifies a particular faulty IGBT. Thus, T1 peak is a group comprising the CWT peaks of coefficient values for different spurious resistance aroused in series with the terminal at IGBT T1. Similarly, it is found distinct and separate clusters are formed by the CWT features in the scatter plot corresponding to faults in different IGBTs. Thus, location of a feature point due to any unknown fault within any of these clusters can provide clear indication about the IGBT where the fault has taken place.

V. CONCLUSION

The present study helps to distinguish healthy from faulty situation and to segregate different faulty situations from each other in a PWM -VSI used for driving induction motors. Features extracted by performing CWT on PVAC of 3-phase line currents of the inverter have been found to form definite clusters in a 3-D scatter plot corresponding to faults in different IGBTs. This study can be extended for faulty situation arising in multiple IGBTs. Validation of the proposed idea will be done in future with practical experimental data.

REFERENCES

[1] K. Rothenhagen and F. W. Fuchs, "Performance of diagnosis methods for IGBT open circuit faults in voltage source active rectifier", in Proc. 35th IEEE Annual Power Electronics Specialists Conference, vol. 6, pp. 4348-4354, 2004

[2] Kastha D. and Bose B.K., "Investigation of fault modes of voltage-fed inverter system for induction motor drive.", IEEE Trans. Ind. Appl., vol 30, pp. 259-266, 1994

[3] P.J. Chrzan, and R. Szczesny, "Fault diagnosis of voltage-fed inverter for induction motor drive", in Proc. IEEE International Symposium on Industrial Electronics, ISIE '96., vol. 2, pp. 1011-1016, 1996.

[4] V. Fernão Pires, T. G. Amaral, D. Sousa and G.D.Marques, " Fault detection of Voltage-Source Inverter using pattern recognition of the 3D current trajectory", in Proc. IEEE Region 8 International Conference on Computational Technologies in Electrical and Electronics Engineering (SIBIRCON), pp. 617-621, July 2010.

[5] J. Klima," Analytical investigation of an induction motor drive under inverter fault mode operations" IEE Proc.-Electr. Power Appl., Vol. 150, No. 3, 255-262, May 2003.

[6] Jang-Hwan Park, Dong-Hwa Kim, Sung-Suk Kim, Dae-Jong Lee and Myung-Geun Chun, "C-ANFIS based fault diagnosis for voltage-fed PWM motor drive systems" In Proc. IEEE Annual Meeting of Fuzzy Information Processing, NAFIPS '04, vol. 1, pp. 379-383, 2004.

[7] Demba Diallo, Mohamed El Hachemi Benbouzid, Denis Hamad, and Xavier Pierre, "Fault detection and diagnosis in an induction machine drive: A pattern recognition approach based on concordia stator mean current vector", IEEE Trans. on Energy Conversion, vol. 20, no. 3, pp. 512-519, 2005.

[8] Abdesh M., Khan S.K., Azizur Rahman M., "A new wavelet based
diagnosis and protection of faults in induction motor drives", in Proc. IEEE Power Electronics Specialists Conference, 2008. pp. 1536-1541, 2008.

[9] Aktas M., Turkmenoglu V., "Wavelet-based switching faults detection in direct torque control induction motor drives", In Proc. IET Science,Measurement & Technology, vol. 4, no. 6, pp. 303-310, 2010.
Hamid Nejjari and Mohamed El Hachemi Benbouzid, "Monitoring and diagnosis of induction motors electrical faults using a current Park's Vector pattern learning approach", IEEE Trans. on Industry Applications, vol. 36, no. 3, pp. 730–735, 2000.
S. Das, C. Koley, P. Purkait, and S. Chakravorti, "Wavelet aided SVM Classifier for stator inter-turn fault monitoring in induction motors", in Proc. IEEE PES General Meeting, USA, pp. 1-6, 2010.
C. Koley, P. Purkait and S. Chakravorti, "Wavelet-Aided SVM Tool for impulse fault identification in transformers", IEEE Trans. Power Delivery, vol. 21, no.3, pp. 1283 -1290, 2006. Robi Polikar, Wavelet Tutorial Part-I, II and III, [Online], Available http://users.rowan.edu/~polikar/WAVELETS/WTpart1.html